Enhanced efficiency of a continuous-wave mode-locked Nd:YAG laser by compensation of the thermally induced, polarization-dependent bifocal lens

N. U. Wetter, E. P. Maldonado, and N. D. Vieira Jr.

Measurements of the bifocal, thermally induced lenses of a cw Nd:YAG laser were obtained. We observed four different focal lengths that are polarization and direction dependent. The focal lengths were used to design stable resonators with large fundamental mode filling in the laser gain medium. The beam is totally polarized in the desired direction even without an intracavity Brewster window. We developed a general approach for the optimization of single-lamp, cw-pumped Nd:YAG lasers. Up to 22 W of cw output power in the vertically polarized TEM_{00} mode and 15 W in the horizontal polarization are obtained for moderate lamp currents. Also, we demonstrate mode locking with 56-ps pulse duration at 33 A of lamp current and up to 13 W of average output power.

Key words: Solid-state lasers, thermal lensing, mode locking.

Introduction

Continuous-wave mode-locked Nd:YAG lasers are widely used in pulse compression experiments in optical fibers and as pumping sources for color center lasers.[1,2,3] All these applications need high stability and output power in the TEM_{00} mode. In spite of its being a well known and important laser system, only recently has it become possible to increase the output power and stability of the fundamental mode TEM_{00} at no expense to pump power.[4] Because of the thermal load in the laser rod produced by the lamp pumping, there is a thermally induced lens (f) in the gain medium. High stability and output power were achieved by increasing the fundamental mode volume within the laser rod, considering the thermally induced lens as an internal optical element in the resonator design. Nevertheless commercial configurations usually use small-diameter beams in the active region to diminish the effects of thermally induced birefringence and spatial variation of the beam mode. Resonators with large mode volume can be specially designed to compensate for some of these effects.[6-9]

Magni *et al.*[10-13] demonstrated that for any resonator with an internal dynamical lens, there are two distinct stability zones ($0 < g_1 g_2 < 1$) corresponding to two different sets of values of f. Around the minimum value of the beam radius in the laser rod, in each of these stability zones, the dependence of the beam radius with f is negligible. In the case of thermally induced focal length this means a large range of pump powers. In these zones, the resonator remains stable and shows little output power fluctuation. In the research of Magni *et al.*, optimization was achieved for a single polarization.

However, Koechner[5] has shown that there are two thermally induced, polarization-dependent focal lengths in the rod. Assuming a cylindrical symmetry for uniform pumping and cooling, there is a focal length for the radial polarization of light (f_R) and a different focal length for tangential polarization (f_T). If we define the parameter α as

$$\alpha = f_T/f_R, \tag{1}$$

α can be calculated by considering the appropriate photoelastic coefficients of Nd:YAG; the theoretical value of α is 1.2. The experimental values are in the range between 1.35 and 1.5.[5]

Thermal Lens Analysis

The laser under investigation is a commercial model[14] polarized by an intracavity Brewster plate. The rod

The authors are with the Instituto de Pesquisas Energéticas e Nucleares, CNEN-SP, P.O. Box 11,049 Pinheiros, Sao Paulo, Brazil 05499.

Received 7 July 1992.
0003-6935/93/275280-05$06.00/0

is a Nd:YAG crystal with dimensions 4 mm × 78 mm, pumped by a single lamp. Both rod and lamp are placed on the foci of a gold-coated elliptical cavity, with the major axis in the horizontal plane.

To measure the polarization- and direction-dependent focal lengths, an aperture with two small rectangular slits was introduced just before the laser rod. The reason for the use of two slits is twofold: it avoids the central part of the rod, where all the foci coincide, and provides the crossover of the two beams for precise determination of the focus. An expanded, collimated, and polarized He–Ne beam illuminates uniformly the whole slit area. If the polarization of the He–Ne beam is along the direction of the slits, the thermal lens for radial polarization is measured; if the polarization is perpendicular to the direction of the slits, the thermal lens for tangential polarization is measured as shown by the scheme in Fig. 1. The results of the focal length measurement for different lamp currents are shown in Fig. 2. Also shown is the best fit considering that f depends on the inverse of the lamp pump power. It is clearly seen that there are four different curves instead of the two expected ones, indicating a spatial asymmetry of the geometrical index profile. It is well known that nonuniform pumping gives nonuniform lensing. In our case, a higher thermal gradient in the horizontal direction is expected because of the closer proximity of the rod to the pump lamp. The focal lengths of the polarization components are related by a function of the lamp current, $\beta(I)$. Therefore we have

$$f_R{}^V = \beta(I) \times f_R{}^H, \tag{2}$$

and accordingly,

$$f_\Phi{}^H = \beta(I) \times f_\Phi{}^V. \tag{3}$$

Combining the effects of axially symmetrical birefringence, α, and the nonuniformity of the thermal

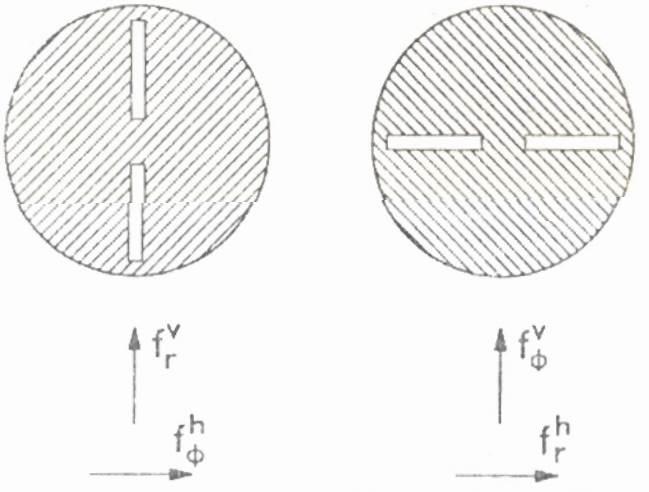

Fig. 1. Rectangular apertures used for measuring the different focal distances f_Φ and f_R for horizontal (h) and vertical (v) polarization directions of the He-Ne beam. The lamp and rod are contained in the horizontal plane.

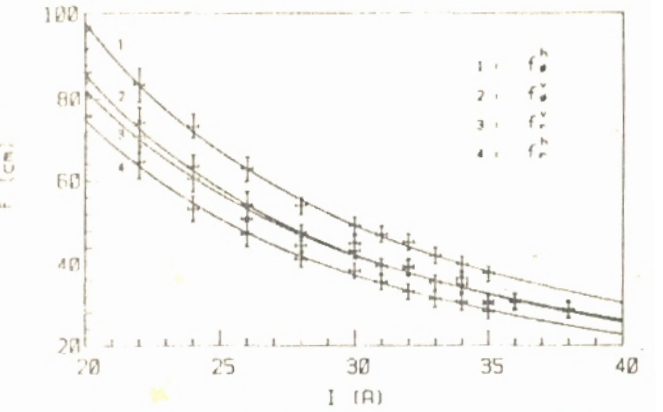

Fig. 2. Measured values of the focal distances for the different polarizations as a function of the lamp current. The lamp voltage is 127 V.

gradient, $\beta(I)$, we now can explain the observed difference between the factors correlating f_Φ and f_R in the horizontal and vertical polarization. By combining expressions 1, 2, and 3 we obtain

$$f_\Phi{}^H = \alpha \times \beta(I) \times f_R{}^H, \tag{4}$$

$$f_\Phi{}^V = \frac{\alpha}{\beta(I)} \times f_R{}^V. \tag{5}$$

By analyzing Fig. 2, we note that $f_\Phi{}^V$ and $f_R{}^V$ show approximately the same value for lamp currents from 28 A up to 38 A. In the case of horizontal polarization we measured a constant ratio of $f_\Phi{}^H$ to $f_R{}^H$ of 1.35. Therefore, $\alpha = \beta$ and $\alpha \times \beta = 1.35$ for lamp currents within this range. Thus α is 1.18, which is in good agreement with the theoretical prediction of $\alpha = 1.2$.

Optimization of the Resonator Design

The idea of increasing the mode volume and maintaining high stability, developed by Magni *et al.*,[10–13] will be followed here, but different, polarization-dependent focal distances are considered.

As is well known, the TEM_{00} spot size inside the rod, w_3, is a function of the following resonator parameters (see Fig. 3): L_1, the rod to back mirror distance, L_2, the rod to front mirror distance, R_1 and R_2, the back and front mirror radii, and the thermal lengths ($f_{R,\Phi}$), according to Eq. (6):

$$w_3(R_1, R_2, L_1, L_2, f_{R,\Phi}) = \hat{w}_3. \tag{6}$$

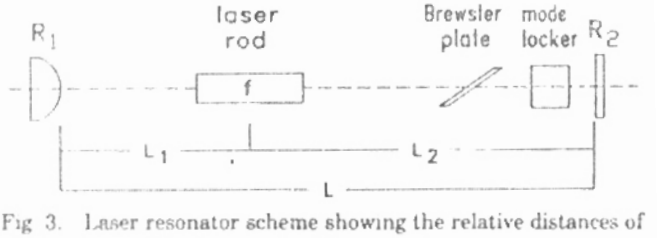

Fig. 3. Laser resonator scheme showing the relative distances of the mirrors and the laser rod. These are the parameters used for high-power optimization.

imposing minimum, thermally induced variation of the TEM_{00} spot size inside the rod, we obtain the following constraint:

$$\frac{\partial}{\partial f_{R,\Phi}} w_3(R_1, R_2, L_1, L_2, f_{R,\Phi}) = 0. \quad (7)$$

As will be shown by our experimental results, the laser remains stable for a large range of pump powers in the neighborhood of the chosen induced thermal lens,

$$f_{R,\Phi} = \hat{f}_{R,\Phi}. \quad (8)$$

To design the desired system, one generally imposes a fixed total resonator length,

$$L_1 + L_2 = \hat{L}, \quad (9)$$

or one gives priority to an available mirror set,

$$R_1 = \hat{R}_1, \quad (10)$$

$$R_2 = \hat{R}_2, \quad (11)$$

where $\hat{w}_3$, $\hat{f}_R$, $\hat{f}_\Phi$, $\hat{R}_1$, $\hat{R}_2$, and $\hat{L}$ are the chosen laser parameters. Generally it is possible to find a satisfactory compromise among Eqs. (9), (10), and (11) as is shown by our experimental configurations.

Another parameter also used in the choice of the optimum resonator is the misalignment sensitivity, $S(R_1, R_2, L_1, L_2, f)$. This parameter is defined in Ref. 10. Small values of S correspond to high stability.

It was found experimentally (we tested several resonator configurations) that to obtain a clean and round beam shape one should use ratios of rod diameter (r) to TEM_{00} spot size (w_3) of the order of $2.0 < r/w_3 < 2.2$ at the chosen input power range (approximately 4 kW). This ratio still prevents higher-order modes from oscillation and minimizes the effects of depolarization that are due to birefringence stress that leads to distortion of the beam shape. In particular, this effect becomes stronger in the outer part of the rod. Because of the presence of the polarizing element (the Brewster window) inside the laser, the larger the beam mode in the rod, the higher the internal losses, in the presence of Brewster windows.[15] Therefore there is a trade-off between the maximum mode size and the polarization-dependent losses.

Laser Configuration and Characterization for Different Polarizations

Vertical Polarization

The vertical polarization presents the same value for radial and tangential focal lengths ($f_\Phi{}^V$ and $f_R{}^V$), as shown in Fig. 2. A general scheme of the laser configuration is shown in Fig. 3. To optimize the resonator for mode locking, we set the effective length of the cavity to $L = 150$ cm (mode locker frequency 49.95 MHz[16]) and optimized it for a thermal focal length of 40 cm, which corresponds to 31 A of lamp current (refer to Fig. 2). The back mirror radius, R_1, is -40 cm, and the output coupler, R_2, is flat, with a transmission of 12%. The distance L_1 is 54.5 cm. Optimization in higher lamp currents is possible using a different set of mirrors.

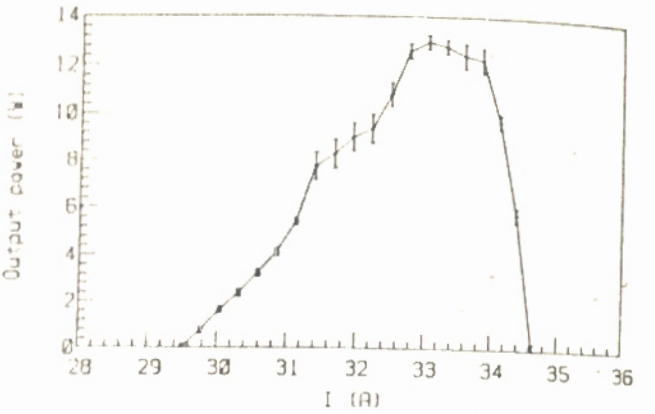

Fig. 4. Average laser output power as a function of the lamp current for the optimized laser configuration in the vertical polarization for an effective resonator length of 150 cm. The error bars indicate the observed fluctuation.

Figure 4 shows the cw output power as a function of the lamp current for the complete configuration, i.e., with the mode-locker inserted. The shift between the expected (31 A) and obtained (33 A) optimum current may be justified by a possible nonoptimum choice of the filling ratio ($r/w = 2.2$) for this polarization. In mode-locked operation an average output power of 13 W was measured. The mode-locked pulses were monitored with a high-speed photodiode[17] (rise time 35 ps) attached to a sampling scope[18] and measured with a background-free autocorrelator. Power measurements were done with a calibrated detector.[19] The autocorrelation trace of the pulses corresponding to 9 W of average power is shown in Fig. 5. Assuming a Gaussian profile, the pulse duration is 56 ps. Decreasing the rf power in the mode locker, the output power increases and the pulse width broadens to 100 ps at 12 W. The

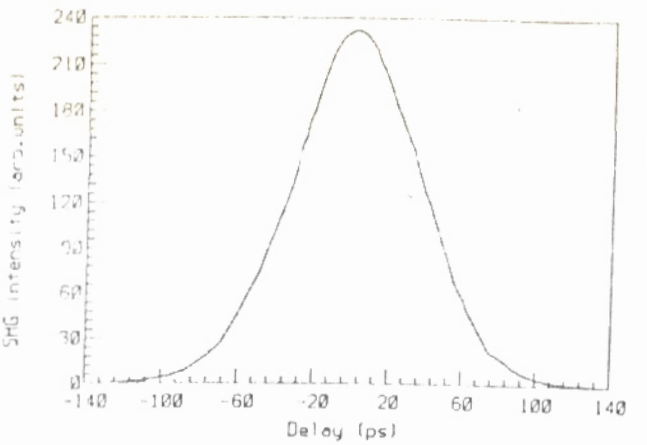

Fig. 5. Background-free second-harmonic generation autocorrelation trace of the mode-locked pulse. Assuming a Gaussian pulse shape, the full width at half maximum is 56 ps

shortest pulse width observed was 50 ps; however, the required rf power (> 5 W) exceeded the capability of the mode-locker system. Typical daily performance is 9 W, with a pulse width of 60 ps (FWHM) and peak-to-peak amplitude fluctuations smaller than 3%, at 33 A of lamp current. For cw operation, without the mode locker, a maximum power of 15 W was obtained at 33 A of lamp current.

To optimize the output power for higher lamp currents and using our set of mirrors, the resonator length was set to 116.8 cm, preserving the distance $L_1 = 54.5$ cm. Pure TEM_{00} mode operation with a maximum output power of 22 W at 35 A of lamp current ($f = 33$ cm) was observed. This means a more than fourfold increase in output power compared with the original commercial configuration[14] at the same input power. The output characteristics are similar to those observed in the mode-locked configuration. Amplitude fluctuations were less than 4%. It is important to point out that, in principle, it should be possible to obtain 22 W for mode-locking operation, with the appropriate set of mirrors for the 1.5-m-long resonator. It should be mentioned that output powers in this range were already achieved for higher lamp pump powers.[4,20]

Horizontal Polarization

In this polarization there are two thermally focal lengths, as shown in Fig. 2. It is of great importance for stable laser output to design resonators where both thermal focal lengths, f_R and f_Φ are at the minimum of the two different stability zones. For a given set of laser parameters, L, f_R, f_Φ, and the chosen mode-filling ratio, Fig. 6 shows the values of $1/R_1$ and $1/R_2$ as a function of L_1 (the rod to the back mirror distance) that optimize the resonator. These calculations were performed following the procedure proposed by Magni,[10] i.e., Eqs. (6)–(11). The curvature of mirror R_1 is independent of the focal length (dashed curve in the figure). The calculations are performed for the two focal lengths, $f_\Phi{}^H$ and $f_R{}^H$, as indicated in the figure. Of course, the values of R_2 that stabilize the laser for each focal length are quite different. However, there are some values of R_2 that will optimize the resonator for both focal lengths, $f_\Phi{}^H$ and $f_R{}^H$, simultaneously (shown by the arrows in Fig. 6). In this case, the focal lengths $f_\Phi{}^H$ and $f_R{}^H$ correspond to the same stable TEM_{00} spot size in the rod.

In our case, the resonator overall length is 117.6 cm; the output coupler radius is $R_2 = -120$ cm, and its transmission is 12%. The focal lengths at 34 A (lamp current) are $f_R{}^H = 30$ cm and $f_\Phi{}^H = 40$ cm. To optimize simultaneously both thermal focal lengths, the calculated mirror radius would have to be $R_1 = -34$ cm, for the distance $L_1 = 40.9$ cm. The available mirror radius was $R_1 = -40$ cm, with 100% reflection at 1.064 nm. At the optimized current the resonator is unstable for the vertical polarization.

The behavior of the laseer output power as a function of the lamp current is shown in Fig. 7. We obtained 15 W of output power at 35 A of lamp current, which corresponds to the calculated optimum configuration lamp current. Stability was better than 3% for cw operation at this current, which shows that the optimization was successful. Rather than the elliptical beam shape that one would expect as a result of the different thermal lenses, we obtained a completely circular beam shape for the polarized TEM_{00} mode, as verified at various distances from the output coupler. This result can be explained by examining the beam profile inside the resonator. The change in focal length of the rod affects the resonator beam profile mostly in the region between the rod and the back mirror and only slightly in the front mirror. The calculated output beam radius for $f = 30$ cm is 395 μm and for $f = 40$ cm is 397 μm at 34 A. In fact, no observed beam asymmetry is seen in all the current range.

A second peak in the output power curve, corresponding to a strongly diffracted TEM_{00} mode with 17 W of output power, is also shown in Fig. 7. We believe that this second peak is due to the use of the back mirror with a value different from the ideal (−40 cm rather than −34 cm). Nevertheless, the good

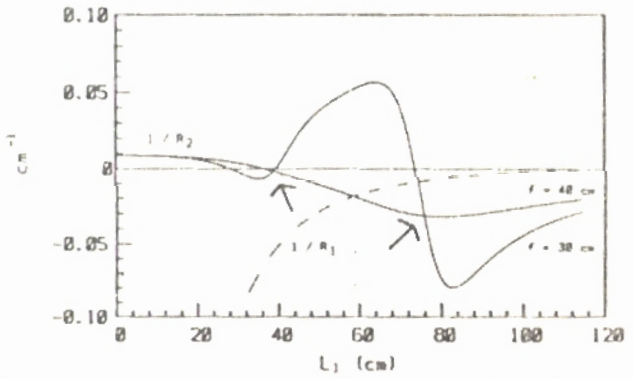

Fig. 6. Values of mirror radius for mode filling corresponding to $r/w_3 = 2.2$ and high stability as a function of the distance (L_1) between the back mirror (R_1) and the rod position. Dashed curves: values of $1/R_1$. Solid curves: values of $1/R_2$ for $f_\Phi{}^H = 40$ cm and $f_R{}^H = 30$ cm. The arrows indicate the values of $1/R_2$ that compensate for both thermal lenses. The cavity overall length is 117.6 cm.

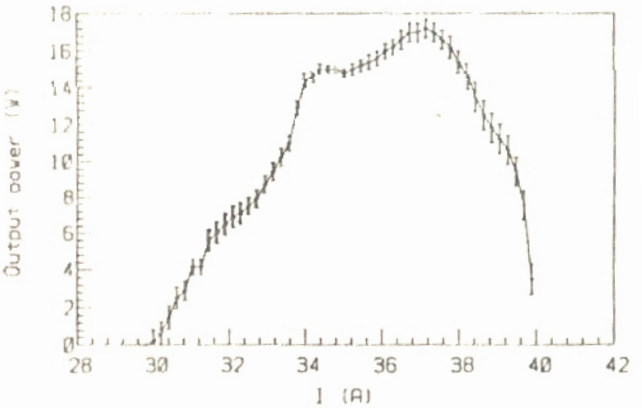

Fig. 7. Output power as a function of the lamp current for the optimized configuration in the horizontal polarization. The error bars indicate the observed fluctuation.

stability of our configuration shows that this method of optimization permits slight changes from the optimized resonator.

At the optimized lamp current, all of the tested laser configurations oscillate in the desired polarization without the Brewster window. This is due to the fact that the thermal lenses of the other polarization directions will not fulfill the stability condition. Without the Brewster window, we observed that when the lamp current is increased, the polarization of the output beam changes between horizontal and vertical. Simultaneously the output power drops to zero at the polarization switching points. Nevertheless the insertion of the Brewster windows ensures that only the desired polarization is dominant in the whole range of lamp currents. The output power is a smooth function of the lamp current, as shown in Figs. 4 and 7, for the desired range of operation.

Conclusions

Measurements of the thermally induced focal lengths of a Nd:YAG rod were made. It was determined that there are four different polarization- and direction-dependent focal lengths. By relating these focal components, it was possible to determine that the coefficient α agrees well with the theoretically predicted value. We configured several resonators, and we considered the measured values of the focal distances to test the predictions of our results. We were able to obtain high output power and good stability in all configurations. In particular, optimized laser performance for the vertical polarization either for cw or for mode-locked operation was demonstrated. Very high cw output power (15 W) at a moderate lamp current (33 A), with a stability of 3% and a typical pulse width of 60 ps in mode-locked operation, was obtained. It is important to note that good stability and beam shape, with a well-defined polarization, are fundamental for a variety of short-pulse applications like pulse compression, synchronous pumping, and additive pulse mode locking. The self-polarizing behavior of our resonators also applies to other materials that lase at different wavelengths for orthogonal polarizations. For example, in Nd:YLF[9] the a axis (σ polarized, 1053 nm) thermal lensing is significantly lower than for the c axis (π polarized, 1047 nm); thus the compensation scheme could wavelength select this laser.

N. U. Wetter is a Ph.D. student under a grant from Coordenação de Aperfeiçoamento de Pessoal de Nível Superior, and E. P. Maldonado is a Ph.D. student under a grant from Fundação de Amparo à Pesquisa do Estado de São Paulo. The project was supported by Fundação de Amparo à Pesquisa do Estado de São Paulo, under grant n 90/3050/5.

References and Notes

1. C. P. Yakymyshyn, J. F. Pinto, and C. R. Pollock, "Additive-pulse mode-locked NaCl:OH laser," Opt. Lett. **14,** 621–623 (1989).
2. A. Finch, X. Zhu, P. N. Kean, W. Sibbett, "Noise characterization of mode-locked color-center laser sources," IEEE J. Quantum Electron. **26,** 1115–1123 (1990).
3. L. Y. Liu, J. M. Huxley, E. P. Ippen, and H. A. Haus, "Self-starting additive-pulse mode locking of a Nd:YAG laser," Opt. Lett. **15,** 553–555 (1990).
4. S. De Silvestri, P. Laporta, and V. Magni, "14-W continuous-wave mode-locked Nd:YAG laser," Opt. Lett. **11,** 785–787 (1986).
5. W. Koechner, *Solid-State Laser Engineering,* 2nd ed. (Springer-Verlag, New York, 1988), Chap. 7, pp. 366–367.
6. L. M. Osterink and J. D. Foster, "Thermal effects and tranverse mode control in a Nd:YAG laser," Appl. Phys. Lett. **12,** 128–131 (1968).
7. F. A. Levine, "TEM_{00} enhancement in a cw Nd:YAG by thermal lensing compensation," IEEE J. Quantum Electron. **QE-7,** 170–172 (1971).
8. R. B. Chesler and D. Maydan, "Convex-concave resonators for TEM_{00} operation of solid-state ion lasers," J. Appl. Phys. **43,** 2254–2257 (1972).
9. H. Vanherzeele, "Thermal lensing measurement and compensation in a continuous-wave mode-locked Nd:YLF laser," Opt. Lett. **13,** 369–371 (1988).
10. V. Magni, "Resonators for solid-state lasers with large-volume fundamental mode and alignment stability," Appl. Opt. **25,** 107–117 (1986).
11. S. Silvestri, P. Laporta, and V. Magni, "The role of the rod position in single-mode solid state laser resonators: Optimization of a cw mode-locked Nd:YAG laser," Opt. Commun. **57,** 339–344 (1986).
12. S. Silvestri, P. Laporta, and V. Magni, "Novel stability diagrams for continuous-wave solid-state laser resonators," Opt. Lett. **11,** 513–514 (1986).
13. S. Silvestri, P. Laporta, and V. Magni, "Misalignment sensitivity of solid-state laser resonators with thermal lensing," Opt. Commun. **59,** 43–48 (1986).
14. Laser Quantronix Model 116, open rail configuration.
15. E. P. Maldonado, G. E. C. Nogueira, and N. D. Vieira, Jr., "Determination of the fundamental laser parameters using an acousto-optical device," IEEE J. Quantum Electron. (to be published).
16. IntraAction Corporation Model 50C, s/n 1683.
17. Opto-Electronics, Inc., Model PD50, s/n 072.
18. Sampling Scope, Tektronix, Model *CSA803, S/N S/B020.*
19. Scientech Power Meter, Model 373, S/N 5022.
20. A. P. DeFonzo, N. Gitkind, C. R. Lutz, and T. A. Kuchta, "High power harmonically mode-locked cw-pumped Nd:YAG laser," Appl. Opt. **27,** 3604–3607 (1988).